Author Manuscript

Author Manuscript

Author Manuscript

Author Manuscript

HHS Public Access

Author manuscript

Acta Biomater. Author manuscript; available in PMC 2016 February 02.

Published in final edited form as:

Acta Biomater. 2015 February ; 13: 188–198. doi:10.1016/j.actbio.2014.11.024.

Manipulation of cellular spheroid composition and the effects on vascular tissue fusion

T.R. Olsen[a], **B. Mattix**[a], **M. Casco**[a], **A. Herbst**[a], **C. Williams**[a], **A. Tarasidis**[a], **D. Simionescu**[a,*], **R.P. Visconti**[c,*], and **F. Alexis**[a,b,*]

[a]Department of Bioengineering, Clemson University, 301 Rhodes Research Center, Clemson, SC 29634, USA

[b]Institute of Biological Interfaces of Engineering, Department of Bioengineering, Clemson University, 401-2 Rhodes Engineering Research Center, Clemson, SC 29634, USA

[c]Department of Regenerative Medicine and Cell Biology, Medical University of South Carolina, 173 Ashley Avenue – BSB 601, Charleston, SC 29425, USA

Abstract

Cellular spheroids were investigated as tissue-engineered building blocks that can be fused to form functional tissue constructs. While spheroids can be assembled using passive contacts for the fusion of complex tissues, physical forces can be used to promote active contacts to improve tissue homogeneity and accelerate tissue fusion. Understanding the mechanisms affecting the fusion of spheroids is critical to fabricating tissues. Here, manipulation of the spheroid composition was used to accelerate the fusion process mediated by magnetic forces. The Janus structure of magnetic cellular spheroids spatially controls iron oxide magnetic nanoparticles (MNPs) to form two distinct domains: cells and extracellular MNPs. Studies were performed to evaluate the influence of extracellular matrix (ECM) content and cell number on the fusion of Janus magnetic cellular spheroids (JMCSs). Results showed that the integration of iron oxide MNPs into spheroids increased the production of collagen over time when compared to spheroids without MNPs. The results also showed that ring tissues composed of JMCSs with high ECM concentrations and high cell numbers fused together, but exhibited less contraction when compared to their lower concentration counterparts. Results from spheroid fusion in capillary tubes showed that low ECM concentrations and high cell numbers experienced more fusion and cellular intermixing over time when compared to their higher counterparts. These findings indicate that cell–cell and cell–matrix interactions play an important role in regulating fusion, and this understanding sets the rationale of spheroid composition to fabricate larger and more complex tissue-engineered constructs.

Keywords

Tissue engineering; Spheroids; Tissue fusion; Magnetic nanoparticles; Magnetic patterning

*Corresponding authors at: Department of Bioengineering, Clemson University, 301 Rhodes Research Center, Clemson, SC 29634, USA. Tel.: +1 864 656 5003; fax: +1 864 656 4466 (F. Alexis). Tel.: +1 864 656 5559; fax: +1 864 656 4466 (D. Simionescu). Tel.: +1 843 792 6024; fax: +1 843 792 0664 (R.P. Visconti). dsimion@clemson.edu (D. Simionescu), visconrp@musc.edu (R.P. Visconti), falexis@clemson.edu (F. Alexis).

Author Manuscript Author Manuscript Author Manuscript Author Manuscript

1. Introduction

A major challenge in tissue engineering is the in vitro fabrication of functional tissue constructs with cell numbers, extracellular matrix (ECM) contents and mechanical properties that mimic the native vasculature [1]. Scaffold-free cellular aggregates, or spheroids, produce their own ECM, allow for precise control over cell number and can fuse into complex tissue structures [2–5]. The stimulation of ECM production and tissue fusion is critical for the fabrication of complex tissue structures using spheroids [5]. The formation of a network of ECM between and throughout adjacent spheroids is critical for structural integrity and provides cues for the fusion process. Tissue fusion is a self-assembly process in which two or more distinct cell populations, or tissues, make contact and coalesce to form a single cohesive structure [3–5]. Factors mediating tissue fusion include cell migration, cell–cell interactions and cell–matrix interactions [3,5,6] to minimize the overall system configurational energy, which results in smaller tissue aggregates [3,7]. Tissue contraction, which includes intracellular cytoskeletal reorganization from cadherin-mediated adhesions, is thought to be responsible for the conformational changes that cause fused tissues of complex geometries to resolve into spheroids over time [8,9].

Conventional tissue assembly and fabrication methods include cell printing, cell sheet techniques and patterned molds [3,4,10,11]. These methods spatially orient the cells and tissues into a desired position to create passive contacts, but do not promote active contact between cells and tissues to accelerate the tissue fusion process. Therefore, the preparation of homogeneous or cohesive engineered tissues remains a challenge when using scaffold-free cellular aggregates. By incorporating magnetic nanoparticles (MNPs) into cellular spheroids, these self-assembled tissues can be aligned and patterned using magnetic force assembly [12–18]. Our lab developed the Janus structure of magnetic cellular spheroids (JMCSs), which provides spatial control of iron oxide MNPs to form two distinct domains: cells and extracellular MNPs [19]. Mattix et al. reported that iron oxide MNPs do not adversely affect the viability of JMCSs and that magnetic forces accelerated the fusion of JMCSs [19]. Unlike conventional tissue patterning methods, magnetic fields are physical forces used to promote active cell–cell contacts and interactions that arise from the adhesive and cohesive interactions between cells under the influence of magnetic attraction [19].

Here, we report our results on manipulating spheroid composition and the effects on JMCS fusion mediated by magnetic forces. The objective of this work was to determine the mechanisms associated with the fusion of JMCSs. The hypothesis driving this work is that spheroid composition, including cell content and ECM content, regulates the fusion kinetics of JMCSs. Our results demonstrate the critical role of cell–cell and cell–ECM interactions for mediating cellular spheroid fusion and show the potential use of magnetic nanoparticles for stimulating ECM production in spheroids.

2. Materials and methods

2.1. Cell culture

Primary rat aortic smooth muscle cells (SMCs) were isolated from the aorta via careful removal of the adventitia and endothelial cell lining, followed by a 1 h incubation with

Author Manuscript Author Manuscript Author Manuscript Author Manuscript

trypsin (0.25%) and collagenase (5 units ml^{-1}). Only passage numbers under ten were used. All cells were cultured in monolayer cultures at 37 ºC and 5% of CO_2 until spheroid assembly. SMCs were cultured using Dulbeco's modified Eagle medium: F-12 (ATCC, 1:1, DMEM:F-12) supplemented with 10% fetal bovine serum (Atlanta Biologics) and 1% penicillin–streptomycin–amphotericin (MediaTech, Inc.).

2.2. Spheroid assembly

Spheroids (Janus magnetic cellular spheroids and non iron oxide spheroids) were prepared using a method developed in our lab and previously described [19–21]. Equal volumes of solutions containing suspended iron oxide MNPs (Fe_3O_4, 20–30 nm, Sky- Spring Nanomaterials, Inc.), collagen (Bovine, Type I, Life Technologies) and cells in cell culture medium were combined and dispensed as hanging drops (15 μl) to form spheroids. Collagen, Type I was prepared according to the manufacturer's recommendations and kept on ice prior to use for all samples. Collagen was only added at the time of spheroid fabrication and not continuously added to the medium. Formulations calling for no collagen were replaced with an equal volume of medium. Unless otherwise noted, all spheroids were incorporated into studies after 3 days of incubation.

2.3. Controlling collagen content during spheroid fabrication

Collagen was only added to spheroids during the fabrication process and not continuously supplemented in the medium. To demonstrate that collagen content within spheroids can be controlled during spheroid formation, histological examination with a Masson's Trichrome stain was used after 3 days of spheroid formation with varying collagen contents (0.017 mg ml^{-1}, 0.1 mg ml^{-1} and 0.25 mg ml^{-1}).

2.4. Viability

PrestoBlue cell viability assays were performed according to the manufacturer's protocol (Life Technologies) in order to quantify cell viability, with at least three repeats per sample. Spheroids were first dissociated via incubation with collagenase (5 units ml^{-1}) (Collagenase Type IV), followed by incubation with trypsin (0.25%) and adherence overnight on a well plate.

2.5. Spheroid sizing

Spheroids with 5000 cells per spheroid and 20,000 cells per spheroid were fabricated and left to form for 3 days. After 3 days, spheroids were imaged using a Nikon AZ100 microscope and their diameters measured using the NIS Elements (Nikon) software package.

2.6. Ring fusion

Spheroid fusion was analyzed by tracking the fusion of spheroids into a ring. Ring magnets were commercially purchased (2 mm external diameter, 1 mm internal diameter, 1 mm thick, Super Magnet Man) and attached to the bottom of a glass chamber slide. 25 individual spheroids of the same formulation were carefully patterned around the ring pattern in a monolayer formation. The low concentration (0.005 mg ml^{-1}) represents a minimal amount

Author Manuscript Author Manuscript Author Manuscript Author Manuscript

of collagen added to spheroids. The high collagen concentration (0.3 mg ml^{-1}) represents the most collagen that could be incorporated into the spheroids and still allow for placement into a ring structure with a lumen. Magnets were removed after 48 h and samples imaged using a Nikon AZ100 multizoom microscope. Four measurements for each ring diameter were recorded (vertical, horizontal and two diagonals) and averaged at each time point. Samples were normalized with themselves, as each sample was analyzed as the percent initial diameter. At least three repeats were performed for each sample.

2.7. Collagen quantification

The collagen content in spheroids was determined using a hydroxyproline assay, as previously described [22]. First, spheroids were hydrolyzed in 4 N sodium hydroxide at 120 ºC for 2 h. Samples were neutralized with 1.4 N citric acid and pH balanced to a range of 7.2 to 7.6. A hydroxyproline standard curve was prepared for calibration of unknown samples. An aliquot of 200 μl was taken from each sample to be incubated with a Chloramine T solution for 15 min and then a *p*-dimethylaminobenzaldehyde solution for 15 min at 65 ºC. Next, experimental samples were prepared as triplicates for optical number readings at 550 nm. Unknown samples were calculated based on the hydroxyproline standard curve. Long term spheroid collagen content studies were normalized to each respective group's collagen content at day 3.

2.8. Capillary tube fusion with varying collagen content and cell numbers

Capillary tubes (500 μm diameter, CTechGlass, CT95-02) were used to study the influence of collagen content and cell number on cellular spheroid fusion. JMCSs composed of primary rat aortic smooth muscle cells were assembled and four of them were placed into capillary tubes full of cell culture medium. The first treatment was varying collagen concentrations incorporated into spheroids, which were 0.017 mg ml^{-1} and 0.24 mg ml^{-1} bovine collagen I (Life Technologies). The low concentration represents the amount of collagen used for making rounded spheroids with some structural support. The high collagen value represents the most collagen that could be incorporated into the spheroids and still allow for placement in the capillary tubes without clogging. For the varying collagen study, 20,000 cells per spheroid were used. The second treatment was varying the cell numbers that were incorporated into spheroids, which were 5000 cells per spheroid and 20,000 cells per spheroid. For the varying cell number study, 0.017 mg ml^{-1} collagen concentration was used. Spheroid filled capillary tubes were placed upright into 0.65 ml polypropylene conical tubes with cell culture medium to allow spheroids to settle to the bottom. Samples were exposed to magnetic forces by placement on top of square magnets (K&J Magnetics, Inc., B881). Immediately after placement into capillary tubes, the spheroids were imaged using an AMG EVOS fl digital inverted microscope to obtain initial diameter measurements of the spheroids using ImageJ. To ensure that no gaps existed between the spheroids and that complete contact existed, the samples were exposed to magnetic forces prior to initial measurements (time = 0 h, Fig. 5A and B). Spheroids were left in capillary tubes for 24 and 48 h prior to further imaging analysis. The 24 and 48 h spheroid measurements were normalized to the initial measurements. At least three repeats were used for each condition to confirm repeatability.

Author Manuscript Author Manuscript Author Manuscript Author Manuscript

2.9. Cellular intermixing

Rat aortic smooth muscle cell solutions were fluorescently labeled using a Vybrant® CFDA SE Cell Tracer Kit (green) or PKH26 Red Fluorescent Cell Linker Kit (red). Stains were performed according to the manufacturer's protocols (Life Technologies). The stained cell solutions were then used to fabricate JMCSs with varying collagen concentrations (0.017 and 0.24 mg ml^{-1}). The low concentration represents the amount of collagen used for making rounded spheroids with some structural support. The high collagen value represents the most collagen that could be incorporated into the spheroids and still allow for placement in the capillary tubes without clogging. Alternating in color, four spheroids were gently placed into capillary tubes (500 μm diameter, CTechGlass, CT95- 02). After 48 h, fluorescent images were captured using a Nikon Ti Eclipse microscope. The ratio view tool on NIS-Elements Software from Nikon Instruments was used to visualize and compare cellular intermixing of the fluorescently labeled spheroids. The ratio view function allows measurement of the ratio of two wavelengths across multiple regions of interest and shows the ratio value by pixel.

2.10. Fusion blocking

To understand the influences of various cell–cell and cell– matrix proteins on spheroid fusion, their functional capacity was inhibited. Four spheroids were gently placed into capillary tubes (500 μm diameter, CTechGlass, CT95-02). Spheroid filled capillary tubes were placed upright into a 0.65 ml polypropylene conical tube with cell culture medium to allow spheroids to settle to the bottom. Samples were exposed to magnetic forces via placement of a square magnet below sample containers (K&J Magnetics, Inc., B881). The medium used in the capillary tubes and conical tube was supplemented with the following in order to inhibit the function of cell–cell and cell–matrix interactions: monoclonal anti-N-cadherin antibody (clone GC-4, Sigma) (40 $\mu g ml^{-1}$), for inhibiting cell–cell interactions regulated by cadherins; and Anti-Mouse/Rat CD29 Functional Grade Purified (eBioscience) (5 $\mu g ml^{-1}$), for inhibiting the cell–matrix interactions of integrin beta 1. After supplementation, spheroids were immediately imaged using an AMG EVOS fl digital inverted microscope and their diameters measured using ImageJ. Fused tissue constructs were then imaged again at 48 h and their lengths measured. Samples were normalized with themselves over time and at least five repeats were used for each treatment. The fusion of the treated samples was compared to the control samples without fusion blockers.

2.11. Histology

All samples were processed and sectioned via paraffin sectioning techniques developed in our lab [23]. Spheroids were fixed, processed (5 μm sections) and stained using either hemotoxylin and eosin (H&E) or Masson's Trichrome stain.

2.12. Statistical analysis

Statistical analyses were performed using an analysis of variance (ANOVA) test to determine if differences were present amongst treatment groups. If differences were determined from the ANOVA, a post hoc two-tailed t-test was used to determine if

Author Manuscript Author Manuscript Author Manuscript Author Manuscript

significant differences existed between treatment groups tested. Error bars on graphs represent the standard deviation from the mean.

3. Results

3.1. Collagen synthesis in JMCSs with MNPs

The development of a viable tissue-engineered construct with mechanical properties similar to native tissues heavily relies on enhancing collagen production. An appealing aspect of cellular spheroids for tissue engineering applications is their ability to dynamically produce their own ECM to meet required mechanical or functional needs of the local environment [2]. Copper and iron ions have been shown to enhance collagen crosslinking in tissues, modulate collagen gene expression and regulate intracellular elastin production, which are critical for the organization and maturation of engineered tissues [24–26]. Patients with beta-thalassaemia and other inherited hemolytic disorders characterized with fluctuations in iron concentration demonstrate defective elastic fibers [26]. Also, it has been shown that iron is associated with gene expression of encoding ECM components [25]. Here, we tested the hypothesis that iron, a physiologically essential nutritional element, could be associated with stimulating production of ECM when iron oxide MNPs are integrated into cellular spheroids.

JMCSs and spheroids without MNPs were fabricated and incubated over 40 days in cell culture medium or cell culture medium supplemented with ascorbic acid (50 $\mu g ml^{-1}$), which is known to stimulate collagen production [11]. Initial collagen concentrations were held constant at 0.017 mg ml^{-1} for spheroids with and without MNPs. Collagen contents of different spheroid types were normalized to each group's respective collagen content at day 3 to eliminate the contribution of the initial collagen added to spheroid during the preparation. Results of hydroxyproline assays qualitatively demonstrate increased collagen production in all spheroid types over time ($P < 0.05$, indicated by "+") (Fig. 1). Results demonstrated that the addition of iron oxide MNPs in JMCSs caused a significant increase in collagen production, when compared to their NIO counterparts at day 40 ($P < 0.05$, as indicated by "_"). Further, the addition of ascorbic acid significantly increased ECM production of both spheroid types ($P < 0.05$, as indicated by "#" for NIO and AANIO and "*" for JMCS and AAJMCS groups). It should be noted that the combination of Janus spheroids with ascorbic acid had a synergistic effect, as the collagen content in these spheroids was significantly greater than in spheroids with ascorbic acid supplementation and no MNPs ($P < 0.05$, as indicated by "="). Compared to day 3, day 40 NIO spheroids had 4.68 times more collagen content, ascorbic-acid-treated NIO spheroids had 6.76 times more collagen content, JMCS spheroids had 6.32 times more collagen content and ascorbic-acid-treated JMCS spheroids had 8.21 times more collagen content. Next, spheroids were histologically sectioned and stained with H&E and Masson's Trichrome stains to visualize nuclei and collagen, respectively, at days 10, 20, 30 and 40 time points (Fig. 1). It is expected that the spheroids containing iron oxide magnetic nanoparticles will be larger in diameter, when compared to spheroids without magnetic particles. To confirm that these two groups contained similar collagen contents at the beginning of the study, a hydroxyproline assay was used to quantify collagen at day 3 for each group. Results showed that although

Author Manuscript Author Manuscript Author Manuscript Author Manuscript

the spheroids differed in size, the collagen content is the same after incorporation of the collagen and MNPs during spheroid formation (Supplemental Fig. S.1). Histological examination suggests that JMSCs and MNP-free spheroids secrete their own collagen, as visually confirmed by an increase in collagen within cellular spheroids over time. As expected, supplementation with ascorbic acid increased collagen production over time in tissue sections. When sectioning spheroids, it is difficult to obtain sections at the same depth in different spheroid populations, which led to the variability in size for tissue sections. Overall, these results demonstrate that iron oxide MNPs stimulate and enhance collagen synthesis when compared to MNP-free controls.

3.2. Collagen synthesis in JMCSs with varying cell numbers

The cell number of a tissue-engineered construct is critical for functionality [3,4,27]. Here, JMCSs with 5000 cells per spheroid and 20,000 cells per spheroid were fabricated and incubated in cell culture medium over 40 days. Initial collagen concentrations were held constant at 0.017 mg ml^{-1} for spheroids with and without MNPs. Collagen contents of different spheroid types were normalized to each group's respective collagen content at day 3. Qualitative results showed that both spheroid types produced collagen over time ($P < 0.05$, as indicated by "+") (Fig. 2). These results indicate that lower cell number spheroids produce similar amounts of collagen, relative to high cell number samples, as there were not significant differences between samples at day 20, day 30 and day 40 time points ($P > 0.05$). The results show that lower cell number spheroids produce more collagen, relative to high cell number samples, as there were significant differences between samples at day 10 ($P < 0.05$, as indicated by "*"). This suggests that the differences in cell number may not be significant after the spheroids are incubated for 10 days or more, which would lead to similar collagen production between the two groups. Spheroids were histologically sectioned and stained with H&E and Masson's Trichrome stains to visualize nuclei and collagen, respectively, at days 10, 20, 30 and 40 time points (Fig. 2). It is expected that the size of the spheroid will be different among 5000 and 20,000 cells per spheroid samples. Spheroids with each cell density were collected after 3 days of formation, imaged and their diameters measured. Results show that 20,000 cells per spheroid samples were significantly larger than the 5000 cells per spheroid counterparts (Supplemental Fig. S.2), which was anticipated due to the presence of more cells. A histological examination demonstrated that both cell densities had cell nuclei through the spheroid and that each saw an increase in collagen production over time, as seen by the increase in blue staining throughout the samples from the Masson's Trichrome stain. Again, the variability in the size of the spheroid sections can be attributed to the difficulty in sectioning spheroids at the same depth amongst different spheroid groups.

3.3. Factors affecting spheroid ring fusion and contraction

To drive the fusion process for the self-assembly of complex tissues, tissue spheroid building blocks must be in direct contact [4]. Morgan's lab reported modeling fusion kinetics of tissue toroids over time, which were fabricated from cell solutions [8,28]. Here, the roles of cell number and ECM content were evaluated for their potential to influence the fusion of cellular spheroids into a tissue ring. 25 JMCSs were patterned on ring magnets and left to fuse for 48 h prior to removal of the magnetic forces. After removal of the magnetic

Author Manuscript Author Manuscript Author Manuscript Author Manuscript

template, two phenomena occur: fusion and contraction. The individual spheroids in the tissue rings will continue to fuse together, while the ring tissue as a whole will contract, or resolve to a rounded spheroid, due to forces generated through cell–cell adhesions and actin networks [8,9,29]. Images of assembled tissue rings were taken daily and the contraction was quantitatively tracked. Complete fusion and contraction was defined as a lack of a lumen within the tissue ring.

First, the influence of cell number was analyzed with samples both with and without ECM. In the presence of ECM (0.017 mg ml^{-1} collagen added during fabricaiton), results indicated that lower cell numbers, 5000 cells per spheroid tested here, showed the fastest and most complete fusion and contraction over 156 h when compared to higher cell numbers, 20,000 cells per spheroid tested here (84 h, 108 h, 132 h and 156 h; $P < 0.05$, as indicated by "*") (Fig. 3a). Visual analysis confirmed that low cell number rings corresponded to the most complete and accelerated fusion and contraction compared to their higher cell number counterparts (Fig. 3b).

Next, the effect of ECM content on ring fusion and contraction was studied by varying the collagen content added to cellular spheroids during fabrication, while holding the cell number constant (20,000 cells per spheroid). To demonstrate that collagen content within spheroids can be controlled during spheroid formation, histological examination with a Masson's Trichrome stain was used after 3 days of spheroid formation with varying collagen contents added. Results of the stain showed an increase in royal blue color throughout the spheroid as the amount of collagen added during spheroid formation was increased from 0.017 mg ml^{-1} to 0.1 mg ml^{-1} to 0.25 mg ml^{-1} (Supplemental Fig. S.3a). Presto blue viability assays confirmed that the addition of collagen content had no adverse effect on spheroid viability at 1 week in rat aortic smooth muscle cells and fibroblasts, when compared to spheroids without collagen added during spheroid formation (Supplemental Fig. S.3b). Results of ring studies showed that lower collagen contents (0.005 mg ml^{-1}) demonstrated the fastest and most complete fusion and contraction when compared to higher collagen spheroids over time (0.3 mg ml^{-1}) (84 h, 108 h and 132 h; $P < 0.05$, as indicated by "*") (Fig. 4a). Visual analysis highlighted the differences in fusion and contraction characteristics based on collagen content (Fig. 4b).

3.4. Spheroid fusion and cellular intermixing in capillary tubes

To study the influence of collagen on spheroid fusion, 0.017 mg ml^{-1} and 0.24 mg ml^{-1} collagen concentrations were used with 20,000 cells per spheroid and 0.3 mg ml^{-1} iron oxide. To study the influence of cell number on spheroid fusion, 5000 and 20,000 cells per spheroid were used with 0.017 mg ml^{-1} collagen and 0.3 mg ml^{-1} iron oxide. Spheroid filled capillary tubes were exposed to magnetic forces via placement of a square magnet below sample containers. Results demonstrate that low collagen JMCSs (0.017 mg ml^{-1}) fused into a more cohesive tissue at 24 and 48 h time points, as the tissue construct sizes were 71% and 65% of initial tissue sizes, respectively (Fig. 5a). High collagen spheroids (0.3 mg ml^{-1}) experienced minimal fusion, as the tissue construct sizes were 93% and 97% of initial tissue sizes at 24 and 48 h time points, respectively. Upon examining the images for low and high collagen groups, the low collagen group tissue construct size was

Author Manuscript Author Manuscript Author Manuscript Author Manuscript

statistically significantly lower at both time points when compared to the high collagen group ($P < 0.05$, as indicated by "*").

Results demonstrate that low cell number spheroids had fused into constructs that were 81% and 68% of initial sizes at 24 and 48 h time points, respectively (Fig. 5b). High cell number spheroids had fused into constructs that were 66% and 59% of initial sizes at 24 and 48 h time points, respectively, which was statistically significantly lower than the 5000 cells per spheroid group at the 24 h time point ($P < 0.05$, as indicated by "*"). These results suggest that low collagen content allows for more cell–cell interactions and cell contraction, and ultimately faster and more complete fusion. With an increase in collagen content, cells become enmeshed in the dense collagen network and their mobility is limited. This prevents the formation of cell–cell adhesions, which are critical to the fusion process. As the cell number increases and collagen content remains constant, there are more opportunities for cell–cell interactions and contacts, which is conducive to promoting faster and more complete fusion in a smaller amount of time. Spheroids with lower cell numbers provide an environment that allows for cells to be mobile and make new cell–cell adhesions, but there are not as many of these contacts due to the lower cell number and this could delay the fusion of tissues.

A hallmark of tissue fusion is cellular intermixing to create a homogeneous tissue [9]. Here, we measured the influence of collagen content and cell number on cellular intermixing during spheroid fusion in capillary tubes. Spheroids with varying collagen content and cell number were fluorescently labeled and allowed to fuse for 48 h in capillary tubes with magnetic forces prior to imaging. Results demonstrated that high collagen (0.24 mg ml^{-1}) spheroids experienced minimal cellular intermixing (8.6%), as demonstrated by the lack of intermixing of fluorescent signal using the ratio view tool in NIS-Elements software (Fig. 6). Low collagen (0.017 mg ml^{-1}) spheroids exhibited significantly more cellular intermixing (22.1%) between adjacent spheroids, as demonstrated by the mixing of fluorescent signal ($P < 0.05$, as indicated by "*"). These results indicate that collagen content influences cellular intermixing and cell migration, which is critical for the fusion process. While collagen content may provide the structural support required for developing tissues, these results indicate that collagen can slow cellular intermixing and migration, both of which are critical to tissue fusion.

Results from studying the influence of varying cell number on spheroid cellular intermixing demonstrated that low cell number spheroids experienced minimal cellular intermixing (10.1%), as demonstrated by the lack of intermixing of the fluorescent signal using the ratio view tool in NIS-Elements software (Fig. 7). High cell number spheroids had significantly more cellular intermixing (22.1%) between adjacent spheroids, as demonstrated by the mixing of the fluorescent signal ($P < 0.05$, as indicated by "*"). These results indicate that the cell number influences cellular intermixing and cell migration, which are both important during the fusion process.

3.5. Cell–cell and cell–matrix interactions influence tissue fusion

The biological relevance of self-assembly of spheroids [30] and even the forces driving the self-assembly of tissue [31] have been reported. However, there is a gap in the literature

Author Manuscript Author Manuscript Author Manuscript Author Manuscript

regarding the influence of cell–cell and cell–matrix proteins on tissue fusion. Work by Lin et al. describes studying the effect of cadherins and integrins during spheroid formation using hepatoma spheroids, yet not much is known about the role of integrins and cadherins during spheroid fusion [32]. To study cell–cell interactions in fusing spheroids, we tested the inhibition of cadherins, which are a family of glycoproteins involved in calcium-dependent cell adhesion. Studies have shown that inhibition with anti-cadherin antibodies induced dissociation of two-dimensional cell layers [33]. Integrins are major adhesion receptors and span across the cell membrane. They are responsible for regulating cell–ECM binding and making transmembrane connections to the cytoskeleton to activate intracellular signaling pathways. The concentrations of cadherin and integrin blockers were 40 $\mu g ml^{-1}$ and 5 $\mu g ml^{-1}$, respectively, which are comparable to work using blockers in studies with forming spheroids by Lin [32] and toroids by Youssef et al. [31]. Results demonstrated that spheroids with functional inhibition of cadherins exhibited tissue construct sizes that were 81% of the initial sizes after 48 h (Fig. 8). For cell–ECM interactions, results showed that spheroids with functional inhibition of integrins exhibited tissue construct sizes that were 85% of the initial sizes after 48 h (Fig. 8). Control spheroids without fusion inhibition had tissue construct sizes that were 68% of the initial, and these results were statistically significantly smaller ($P < 0.05$, as indicated by "*") than both the anti-cadherin and anti-integrin spheroids, which demonstrates that cell–cell and cell–matrix proteins do play a role in tissue fusion. However, significant differences were not observed between the influences of cadherins and integrins, which suggests that both cell–cell and cell–matrix interactions are involved in fusion and that other cell–cell and cell–matrix protein blockers still need to be tested. These results add to the understanding of the complex mechanisms behind tissue fusion and show the potential for future tissue fabrication experiments to be tailored using optimal spheroid formulations for rapid and complete tissue fusion.

4. Discussion

In this work, we have demonstrated that iron oxide MNPs stimulate the synthesis of collagen in cellular spheroids, when compared to no iron oxide control spheroids. This stimulation is perhaps due to the interactions of cells on the surface of the nanoparticles or release of iron ions during degradation in the spheroid [20]. Further, our results show that the influences of iron oxide on collagen synthesis are similar to that of ascorbic acid, a known collagen synthesis stimulant. Future work will include studying the influence of MNPs on collagen crosslinking and accelerating the maturation of tissues assembled with JMCSs.

Bottom-up engineering approaches, like cell sheet and cellular spheroid techniques, allow for control over the cell number and ECM content. However, the role of cell–cell and cell–ECM interactions on tissue fusion has not been fully understood. Our results demonstrate that the composition of the building block for tissue fabrication is critical because cell number and ECM content mediate the fusion process. The active fusion created from the physical magnetic forces increased cell–cell adhesions, which is perhaps mediated by increased cadherin interactions. This activity may lead to downstream intercellular and intracellular signaling that promotes fusion through cell migration and reorganization, ECM remodeling and cytoskeletal contraction. Future research must involve not only accelerating

Author Manuscript Author Manuscript Author Manuscript Author Manuscript

the fusion of tissues, but also studying the deposition of other ECM proteins, like elastin and fibronectin, and the enhancement of mechanical properties.

Overall, our results show that it is not only the magnetic forces but the composition of the spheroids used that is important to accelerate fusion of spheroids when they are exposed to magnetic forces. Results from tissue ring and capillary studies show that ECM content plays a role in mediating tissue fusion, as higher collagen content decreases the rate of tissue fusion. While high collagen content spheroids may not provide for the most cell intermixing, as seen in Fig. 7, it is critical for providing structural integrity of our tissue at later time points and when building larger tissues as shown in Fig. 4 using rings. In previous work from our lab, fluorescently labeled high collagen tissue tubes that were fused for 24 h showed minimal cell intermixing, as demonstrated by maintained spatial orientation of endothelial cell, smooth muscle cell and fibroblast layers. Our work presented here confirms that minimal cell intermixing is occurring at early time points between adjacent spheroids in capillary tubes. Dvir-Ginzberg et al. showed that the cell number is critical to fabricating liver tissue constructs, as higher cell number spheroids led to increased viability and metabolic output, compared to lower cell numbers [27]. This indicates that using a physiologically relevant cell number is critical not only to tissue formation, but also in defining tissue functionality. Future work will include monitoring the cell number in individual spheroids and fusing spheroids over time, to understand how cell number influences the developing tissues. Our work has shown that the fusion process is regulated by cell– cell and cell–matrix interactions, as inhibition of cadherins and integrins led to less fusion over time, when compared to untreated controls. Our work represents the beginning in understanding how spheroid composition is critical for the fusion of spheroids into complex tissues mediated by magnetic forces. Using this information, more effective and applicable engineered tissues may be developed due to optimized predictions prior to assembly.

5. Conclusions

In conclusion, spheroid composition is critical to the fusion process and manipulation of the composition was utilized to study fusion kinetics of JMCSs mediated by magnetic forces. Results showed that ECM content and cell number play a key role in mediating the fusion of cellular spheroids into complex tissues. The results also showed that iron oxide MNPs in JMCSs stimulate collagen production, which is critical for scaffold-free tissue engineering. Further, results demonstrated that cell–cell and cell–ECM interactions in spheroids are critical in determining the fusion dynamics of tissues. This new understanding of JMCS composition and its influence on fusion can be applied to the fabrication of larger tissues, like blood vessels. This could be a change in paradigm when related to tissue engineering approaches because more collagen does not result in enhanced fusion. Future work will involve using magnetic forces to induce maturation of assembled tissue constructs, with a focus on enhancing ECM production and mechanical properties.

Supplementary Material

Refer to Web version on PubMed Central for supplementary material.

Author Manuscript Author Manuscript Author Manuscript Author Manuscript

Acknowledgments

This work was supported by the American Heart Association Beginning Grant in Aid-2BGIA11720004 award to F.A., the SC EPSCOR Grant for Exploratory Academic Research-2012001188 awarded to F.A., and the NSF/EPSCOR EPS-0447660 award to R.P.V. The authors wish to thank Dr T. Bruce and the Clemson Light Imaging Facility at Clemson University for technical support with microscopy and Mrs L. Jenkins for her help with histological techniques.

References

1. Olsen TR, Alexis F. Bioprocessing of tissues using cellular spheroids. J Bioprocess Biotech. 2014; 4:e112.
2. Kelm JM, Lorber V, Snedeker JG, Schmidt D, Broggini-Tenzer A, Weisstanner M, et al. A novel concept for scaffold-free vessel tissue engineering: self-assembly of microtissue building blocks. J Biotech. 2010; 148:46–55.
3. Jakab K, Norotte C, Marga F, Murphy K, Vunjak-Novakovic G, Forgacs G. Tissue engineering by self-assembly and bio-printing of living cells. Biofabrication. 2010; 2:022001. [PubMed: 20811127]
4. Mironov V, Visconti RP, Kasyanov V, Forgacs G, Drake CJ, Markwald RR. Organ printing: tissue spheroids as building blocks. Biomaterials. 2009; 30:2164–74. [PubMed: 19176247]
5. Pérez-Pomares JM, Foty RA. Tissue fusion and cell sorting in embryonic development and disease: biomedical implications. BioEssays. 2006; 28:809–21. [PubMed: 16927301]
6. Jakab K, Neagu A, Mironov V, Markwald RR, Forgacs G. Engineering biological structures of prescribed shape using self-assembling multicellular systems. Proc Natl Acad Sci USA. 2004; 101:2864–9. [PubMed: 14981244]
7. Jakab K, Norotte C, Damon B, Marga F, Neagu A, Besch-Williford CL, et al. Tissue engineering by self-assembly of cells printed into topologically defined structures. Tissue Eng Part A. 2008; 14:413–21. [PubMed: 18333793]
8. Napolitano AP, Chai P, Dean DM, Morgan JR. Dynamics of the self-assembly of complex cellular aggregates on micromolded nonadhesive hydrogels. Tissue Eng. 2007; 13:2087–94. [PubMed: 17518713]
9. Athanasiou KA, Eswaramoorthy R, Hadidi P, Hu JC. Self-organization and the self-assembling process in tissue engineering. Annu Rev Biomed Eng. 2013; 15:115–36. [PubMed: 23701238]
10. Boland T, Xu T, Damon B, Cui X. Application of inkjet printing to tissue engineering. Biotechnol J. 2006; 1:910–7. [PubMed: 16941443]
11. L'heureux N, Pâquet S, Labbé R, Germain L, Auger FA. A completely biological tissue-engineered human blood vessel. FASEB J. 1998; 12:47–56. [PubMed: 9438410]
12. Bratt-Leal A, Kepple KL, Carpenedo RL, Cooke MT, McDevitt TC. Magnetic manipulation and spatial patterning of multi-cellular stem cell aggregates. Integr Biol. 2011; 3:1224–32.
13. Ho VHB, Müller KH, Barcza A, Chen R, Slater NKH. Generation and manipulation of magnetic multicellular spheroids. Biomaterials. 2010; 31:3095–102. [PubMed: 20045553]
14. Lin R-Z, Chu W-C, Chiang C-C, Lai C-H, Chang H-Y. Magnetic reconstruction of three-dimensional tissues from multicellular spheroids. Tissue Eng Part C: Methods. 2008; 14:197–205. [PubMed: 18781835]
15. Rezende RA, Azevedo FS, Pereira FD, Kasyanov V, Wen X, de Silva JVL, et al. Nanotechnological strategies for biofabrication of human organs. J Nanotechnol. 2012; 2012:1–10.
16. Sasaki T, Iwasaki N, Kohno K, Kishimoto M, Majima T, Nishimura SI, et al. Magnetic nanoparticles for improving cell invasion in tissue engineering. J Biomed Mater Res Part A. 2007; 86:969–78.
17. Shimizu K, Ito A, Arinobe M, Murase Y, Iwata Y, Narita Y, et al. Effective cellseeding technique using magnetite nanoparticles and magnetic force onto decellularized blood vessels for vascular tissue engineering. J Biosci Bioeng. 2007; 103:472–8. [PubMed: 17609164]
18. Shimizu K, Ito A, Honda H. Mag-seeding of rat bone marrow stromal cells into porous hydroxyapatite scaffolds for bone tissue engineering. J Biosci Bioeng. 2007; 104:171–7. [PubMed: 17964479]

Author Manuscript Author Manuscript Author Manuscript Author Manuscript

19. Mattix BM, Olsen TR, Casco M, Reese L, Poole JT, Zhang J, et al. Janus magnetic cellular spheroids for vascular tissue engineering. Biomaterials. 2014; 35:949–60. [PubMed: 24183699]
20. Mattix B, Olsen TR, Gu Y, Casco M, Herbst A, Simionescu DT, et al. Biological magnetic cellular spheroids as building blocks for tissue engineering. Acta Biomater. 2014; 10:623–9. [PubMed: 24176725]
21. Mattix B, Olsen TR, Moore T, Casco M, Simionescu D, Visconti RP, et al. Accelerated iron oxide nanoparticle degradation mediated by polyester encapsulation within cellular spheroids. Adv Funct Mater. 2014; 24:800–7.
22. Blumenkrantz N, Asboe-Hansen G. An assay for hydroxyproline and proline on one sample and a simplified method for hydroxyproline. Anal Biochem. 1975; 63:331–40. [PubMed: 1122021]
23. Olsen TR, Mattix B, Casco M, Herbst A, Williams C, Tarasidis A, et al. Processing cellular spheroids for histological examination. J Histotechnol. 2014
24. Dahl SLM, Rucker RB, Niklason LE. Effects of copper and cross-linking on the extracellular matrix of tissue-engineered arteries. Cell Transplant. 2005; 14:367–74. [PubMed: 16180655]
25. Fathima NN, Rao JR, Nair BU. Effect of UV irradiation on the physico-chemical properties of iron crosslinked collagen. J Photochem Photobiol, B. 2011; 105:203–6. [PubMed: 22000623]
26. Bunda S, Kaviani N, Hinek A. Fluctuations of intracellular iron modulate elastin production. J Biol Chem. 2005; 280:2341–51. [PubMed: 15537639]
27. Dvir-Ginzberg M, Gamlieli-Bonshtein I, Agbaria R, Cohen S. Liver tissue engineering within alginate scaffolds: effects of cell-seeding density on hepatocyte viability, morphology, and function. Tissue Eng. 2003; 9:757–66. [PubMed: 13678452]
28. Livoti CM, Morgan JR. Self-assembly and tissue fusion of toroid-shaped minimal building units. Tissue Eng Part A. 2010; 16:2051–61. [PubMed: 20109063]
29. Martin P, Parkhurst SM. Parallels between tissue repair and embryo morphogenesis. Development. 2004; 131:3021–34. [PubMed: 15197160]
30. Singh A, Dilnawaz F, Mewar S, Sharma U, Jagannathan NR, Sahoo SK. Composite polymeric magnetic nanoparticles for co-delivery of hydrophobic and hydrophilic anticancer drugs and MRI imaging for cancer therapy. ACS Appl Mater Interfaces. 2011; 3:842–56. [PubMed: 21370886]
31. Youssef J, Nurse AK, Freund LB, Morgan JR. Quantification of the forces driving self-assembly of three-dimensional microtissues. Proc Natl Acad Sci. 2011; 108:6993–8. [PubMed: 21482784]
32. Lin R-Z, Chou L-F, Chien C-C, Chang H-Y. Dynamic analysis of hepatoma spheroid formation: roles of E-cadherin and β1-integrin. Cell Tissue Res. 2006; 324:411–22. [PubMed: 16489443]
33. Takeichi M. The cadherins: cell-cell adhesion molecules controlling animal morphogenesis. Development. 1988; 102:639–55. [PubMed: 3048970]

Appendix A. Figures with essential colour discrimination

Certain figure in this article, particularly Figs. 1–8 is difficult to interpret in black and white. The full colour images can be found in the on-line version, at http://dx.doi.org/10.1016/j.actbio.2014.11.024.

Appendix B. Supplementary data

Supplementary data associated with this article can be found, in the online version, at http://dx.doi.org/10.1016/j.actbio.2014.11.024.

Author Manuscript Author Manuscript Author Manuscript Author Manuscript

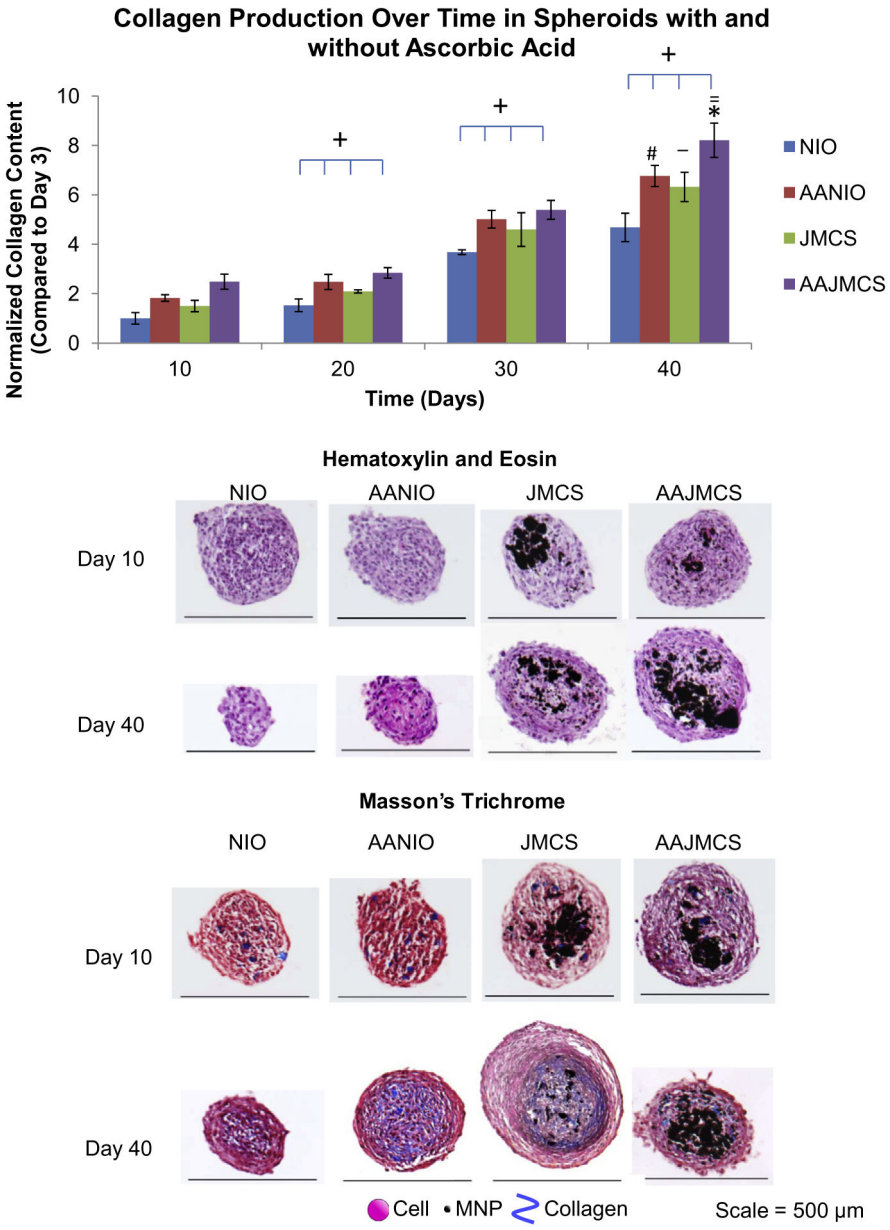

Fig. 1.

Effect of iron oxide MNPs on collagen synthesis within JMCSs. Results of hydroxyproline assays qualitatively demonstrate increased collagen production in NIO, AANIO, JMCS and AAJMCS spheroids over 40 days ($P < 0.05$, as indicated by "+"). Results demonstrated that the addition of iron oxide MNPs in JMCSs caused a significant increase in collagen production, when compared to their NIO counterparts ($P < 0.05$, as indicated by "_"). Further, the addition of ascorbic acid significantly increased ECM production of both spheroid types ($P < 0.05$, as indicated by "#" for NIO and AANIO and "*" for JMCS and AAJMCS groups). It should be noted that the combination of Janus spheroids with ascorbic acid had a synergistic effect, as the collagen content in these spheroids was significantly greater than in spheroids with ascorbic acid supplementation and no MNPs ($P < 0.05$, as

Author Manuscript Author Manuscript Author Manuscript Author Manuscript

indicated by "="). Results of the Masson's Trichrome stain suggest that all spheroid samples secrete their own collagen over time (increase in blue), which indicates that MNPs have no adverse effects on collagen synthesis within cellular spheroids. NIO = no iron oxide, AANIO = ascorbic acid no iron oxide, JIO = Janus iron oxide, AAJIO = ascorbic acid Janus iron oxide.

Author Manuscript Author Manuscript Author Manuscript Author Manuscript

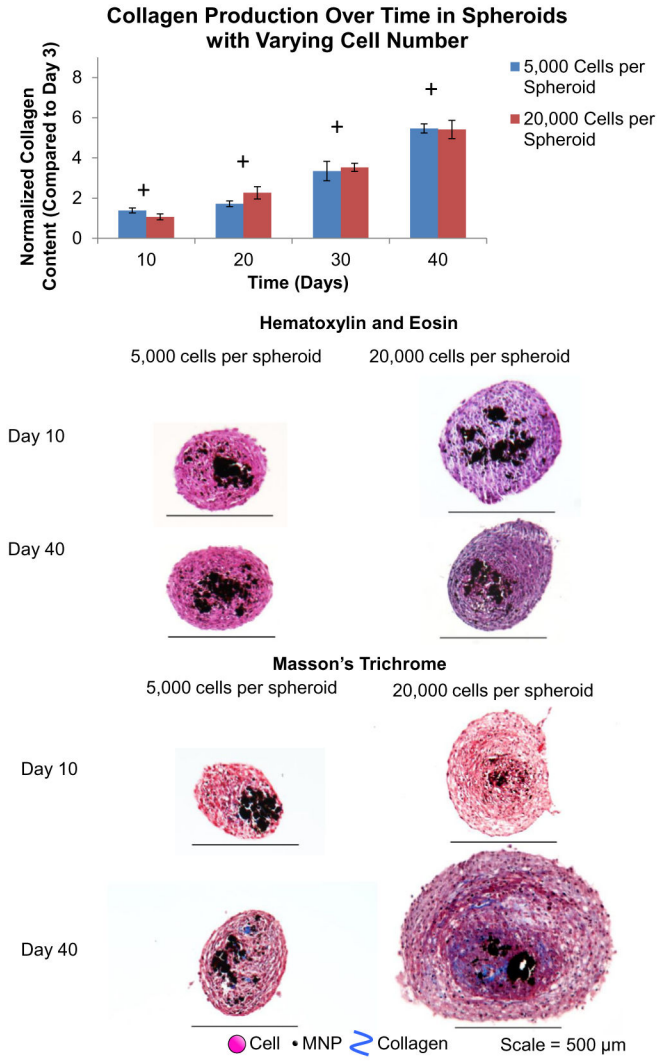

Fig. 2.

Effect of cell number on collagen synthesis within JMCSs. Results of hydroxyproline assays qualitatively demonstrated increased collagen production in spheroids with both 5000 and 20,000 cells per spheroid samples over 40 days ($P < 0.05$, as indicated by "+"). The results indicate that lower cell number spheroids produce similar amounts of collagen, relative to high cell number samples, as there were not significant differences between samples at day 20, day 30 and day 40 time points ($P > 0.05$). The results show that lower cell number spheroids produce more collagen, relative to high cell number samples, as there were significant differences between samples at day 10 ($P < 0.05$, as indicated by "*"). This suggests that the differences in cell number may not be significant after the spheroids are incubated for 10 days or more, which would lead to similar collagen production between the two groups. Results of the Masson's Trichrome stains suggest that all spheroid samples produce their own collagen over time (increase in blue stain), which indicates that cell number has no adverse effects on collagen synthesis within cellular spheroids.

Author Manuscript Author Manuscript Author Manuscript Author Manuscript

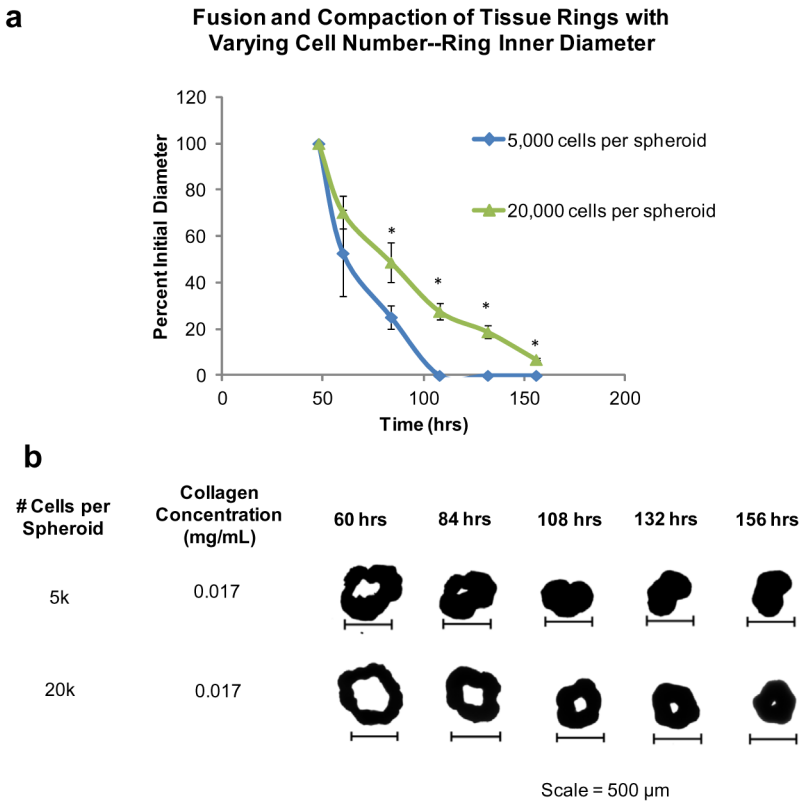

Fig. 3.

Effect of cell number on ring fusion and compaction. Quantification of tissue fusion and compaction over time was performed using rings with JMCSs composed of varying cell numbers and measuring the changes in inner diameter of the rings over time. (a) In the presence of ECM, results show that the lower cell numbers, 5000 cells per spheroid, had the fastest and most complete fusion and compaction, when compared to high cell number spheroids (20,000 cells per spheroid). Four measurements for each ring diameter were recorded (vertical, horizontal and two diagonals) and averaged at each time point. At the 84 h, 108 h, 132 h and 156 h time points the percent initial ring diameters of the 5000 cell spheroids were significantly smaller when compared to the 20,000 cells spheroid counterparts ($P < 0.05$, as indicated by "*"). (b) Visual analysis of ring fusion confirms that cell number does play a role in tissue fusion and compaction, with differences between low and high cell numbers clearly present.

Author Manuscript Author Manuscript Author Manuscript Author Manuscript

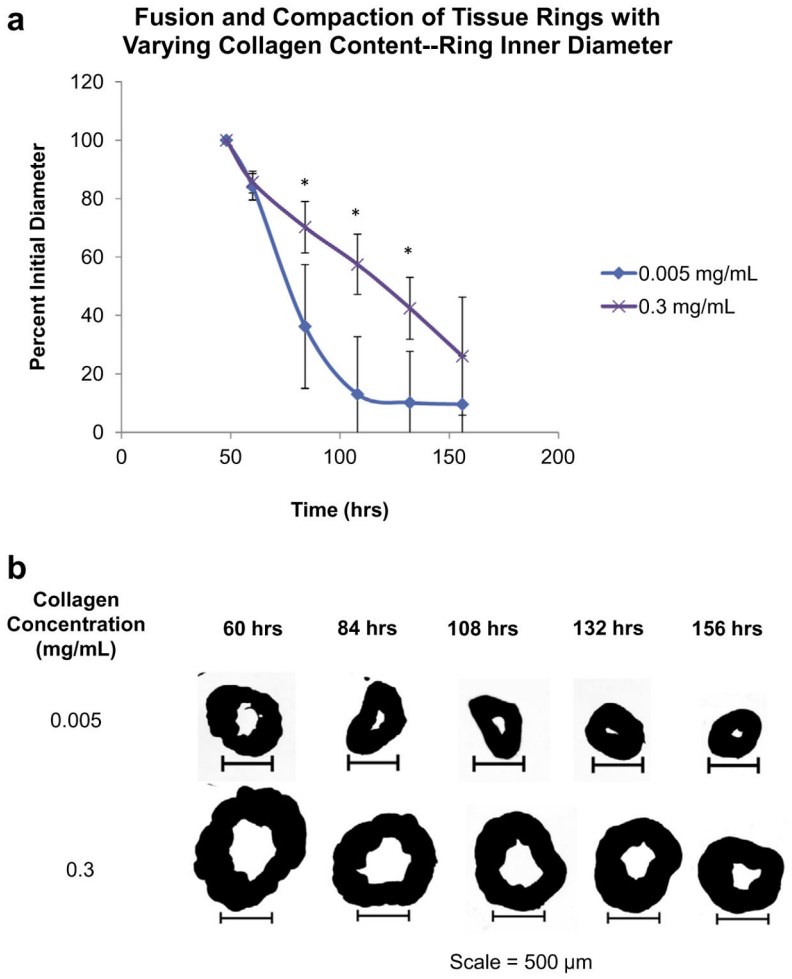

Fig. 4.

Effects of ECM on ring fusion and compaction. The effects of varying collagen contents for tissue fusion and compaction was quantified over time for rings composed of JMCSs with two collagen contents, 0.005 mg ml^{-1} and 0.3 mg ml^{-1}. (a) At the 84 h, 108 h and 132 h time points the percent initial ring diameters of the 0.005 mg ml^{-1} collagen spheroids were significantly smaller when compared to the 0.3 mg ml^{-1} collagen spheroid counterparts ($P < 0.05$, as indicated by "*"). Four measurements for each ring diameter were recorded (vertical, horizontal and two diagonals) and averaged at each time point. (b) Visual analysis of ring fusion confirms that collagen content plays a significant role in tissue fusion and compaction, with decreases in fusion and compaction becoming evident with increasing collagen concentrations.

Author Manuscript Author Manuscript Author Manuscript Author Manuscript

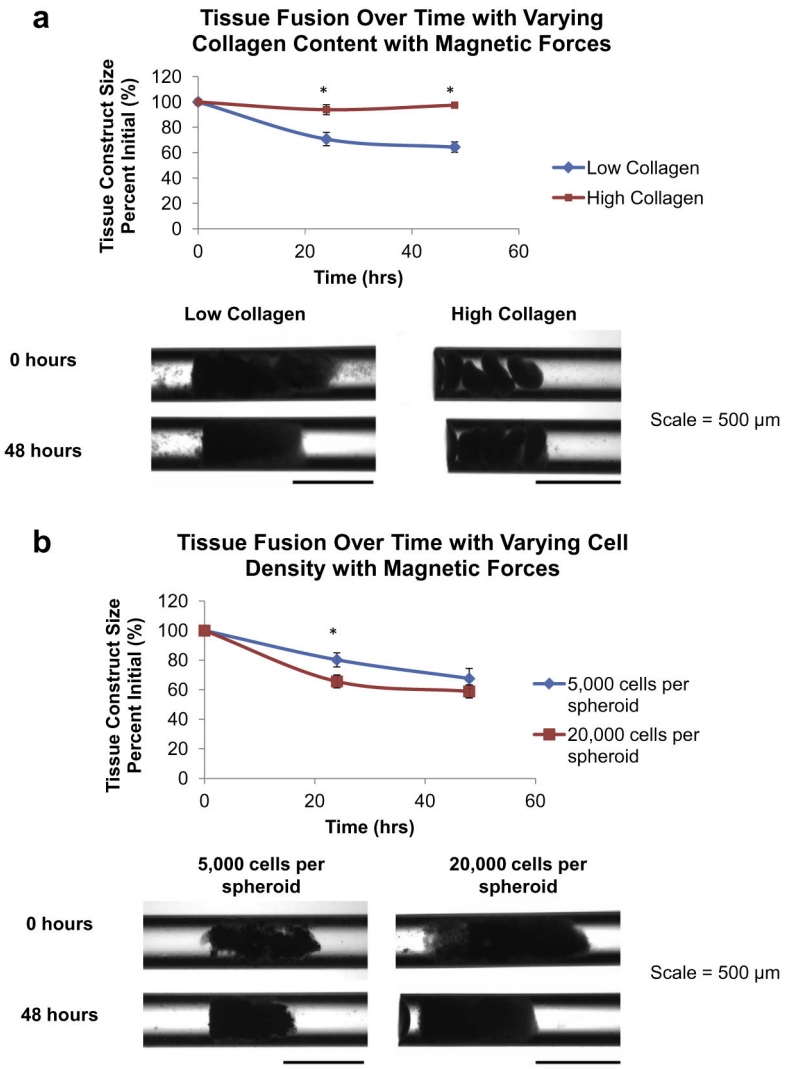

Fig. 5.

Tissue fusion in JMCSs with varying collagen content and varying cell number mediated by magnetic forces. JMCSs were assembled and placed into capillary tubes full of cell culture medium. Samples were exposed to magnetic forces via placement of a square magnet below sample containers. (a) Results demonstrate that low collagen JMCSs (0.017 mg ml^{-1}) fused into a more cohesive tissue at 24 and 48 h time points, as the tissue construct sizes were 71% and 65% of initial tissue sizes, respectively. High collagen spheroids (0.3 mg ml^{-1}) experienced minimal fusion, as the tissue construct sizes were 93% and 97% of initial tissue sizes at 24 and 48 h time points, respectively. At both time points, the tissue construct sizes of the low collagen JMCSs were significantly smaller than the high collagen JMCSs ($P < 0.05$, as indicated by "*"). Visual analysis shows that low collagen spheroids fused into a more homogenous structure after 48 h, while the high collagen spheroids fused minimally and the individual spheroids can still be seen. (b) Results demonstrate that low cell number spheroids (5000 cells per spheroid) had fused into constructs that were 81% and 68% of initial sizes at 24 and 48 h time points, respectively. High cell number spheroids (20,000

Author Manuscript Author Manuscript Author Manuscript Author Manuscript

cells per spheroid) had fused into constructs that were 66% and 59% of initial sizes at 24 and 48 h time points, respectively, which was statistically significantly lower than the 5000 cells per spheroid group at the 24 h time point ($P < 0.05$, as indicated by "*"). Visual analysis shows that both cell types fuse to similar sized constructs after 48 h.

Author Manuscript Author Manuscript Author Manuscript Author Manuscript

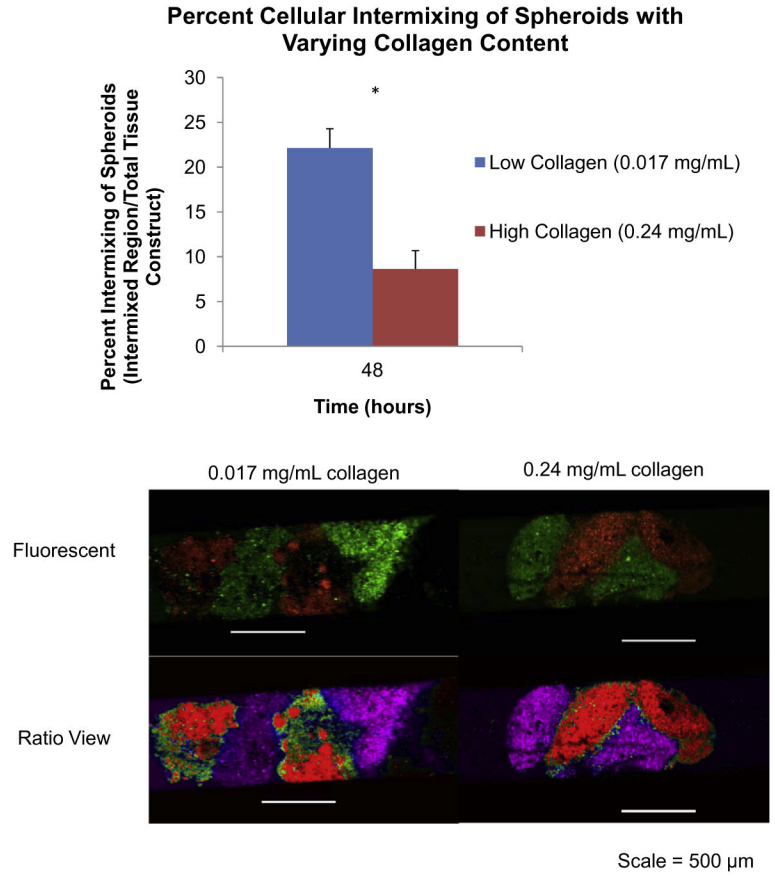

Fig. 6.

Cellular intermixing in JMCSs with varying collagen content. Spheroids with varying collagen content and cell number were fluorescently labeled and allowed to fuse for 48 h in capillary tubes with magnetic forces prior to imaging. (a) Results demonstrated that high collagen (0.24 mg ml^{-1}) spheroids experienced minimal cellular intermixing (8.6%), as demonstrated by the lack of intermixing of fluorescent signal using the ratio view tool in NIS-Elements software. Low collagen (0.017 mg ml^{-1}) spheroids had significantly more cellular intermixing (22.1%) between adjacent spheroids, as demonstrated by the mixing of the fluorescent signal ($P < 0.05$, as indicated by "*").

Author Manuscript Author Manuscript Author Manuscript Author Manuscript

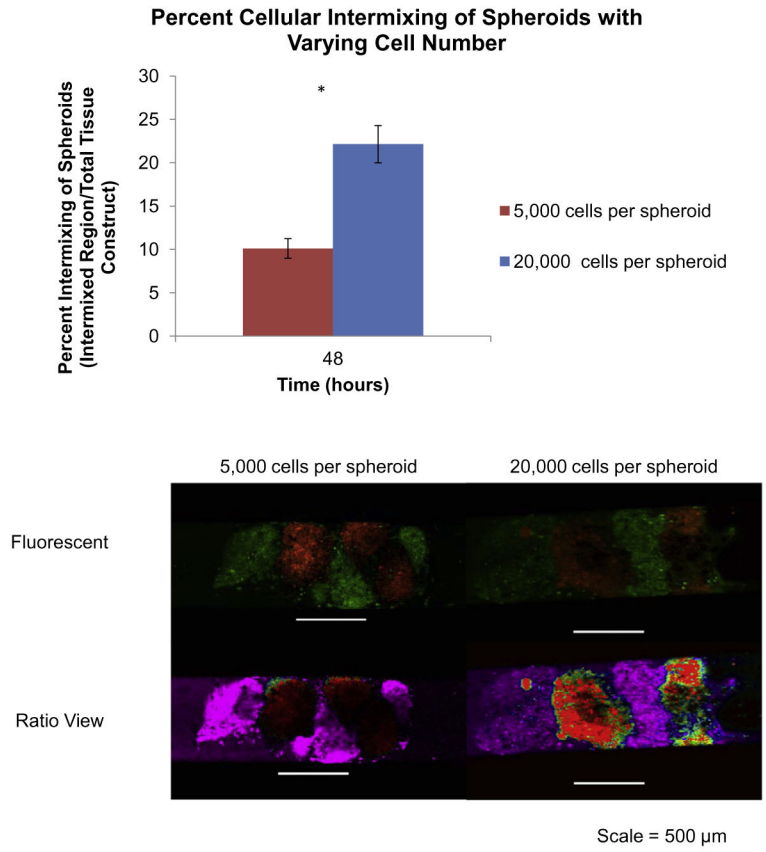

Fig. 7.

Cellular intermixing in JMCSs with varying cell number. Results from studying the influence of varying cell number on spheroid cellular intermixing demonstrated that low cell number (5000 cells per spheroid) spheroids experienced minimal cellular intermixing (10.1%), as demonstrated by the lack of intermixing of fluorescent signal using the ratio view tool in NIS-Elements software. High cell number spheroids (20,000 cells per spheroid) had significantly more cellular intermixing (22.1%) between adjacent spheroids, as demonstrated by the mixing of the fluorescent signal ($P < 0.05$, as indicated by "*"). These results indicate that cell number influences cellular intermixing and cell migration, which are both important during the fusion process.

Author Manuscript Author Manuscript Author Manuscript Author Manuscript

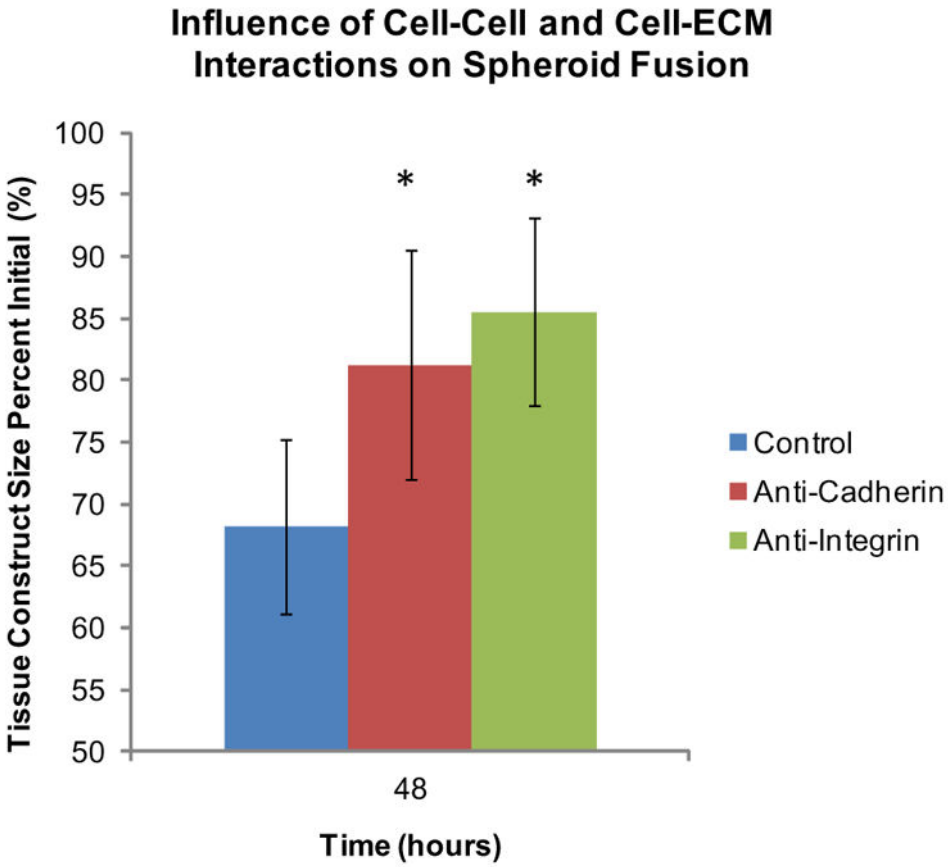

Fig. 8.

Influence of cell–ECM and cell–cell interactions on spheroid fusion. For studying cell–matrix interactions, the function of integrins was inhibited with an anti-integrin functional grade antibody in fusing spheroids in capillary tubes. Results showed that spheroids with functional inhibition of integrins had tissue construct sizes that were 85% of the initial sizes after 48 h. Results demonstrated that spheroids with functional inhibition of cadherins had tissue construct sizes that were 81% of the initial sizes after 48 h. Control spheroids without fusion inhibition had tissue construct sizes that were 68% of the initial, and these results were statistically significantly smaller than anti-integrin and anti-cadherin spheroids ($P < 0.05$, as indicated by "*"), which demonstrates that cell–matrix and cell– cell proteins do play a role in tissue fusion.